Hydrogen physisorption channel on graphene: a highway for atomic H diffusion

H. González-Herrero, E Cortés-del Río, P. Mallet, J.-Y. Veuillen, P Palacios, J Gómez-Rodríguez, I. Brihuega, F. Yndurain

Hydrogen physisorption channel on graphene: a highway for atomic H diffusion

H. González-Herrero[1-3], E. Cortés-del Río[1-3], P. Mallet[4-5], J-Y. Veuillen[4-5], J.J Palacios[1-3], J.M. Gómez-Rodríguez[1-3], I. Brihuega[1-3], F. Ynduráin[1-3].*

[1] Departamento Física de la Materia Condensada, Universidad Autónoma de Madrid, E-28049 Madrid, Spain.

[2] Condensed Matter Physics Center (IFIMAC), Universidad Autónoma de Madrid, E-28049 Madrid, Spain.

[3] Instituto Nicolás Cabrera, Universidad Autónoma de Madrid, E-28049 Madrid, Spain

[4] Université Grenoble Alpes, Institut NEEL, F-38042 Grenoble, France

[5] CNRS, Institut NEEL, F-38042 Grenoble, France

*Correspondence to: ivan.brihuega@uam.es

Abstract

We study the adsorption of atomic hydrogen on graphene by combining scanning tunneling microscopy experiments and first principle calculations. Our results reveal the existence of a physisorption channel over the graphene layer, dominated by van der Waals forces and thus homogeneous over the whole atomic lattice, where atomic hydrogen can move freely. Such physisorption channel is essential to understand the final configuration of hydrogen atoms chemisorbed on graphene. We find that ~ 95% of chemisorbed H atoms form non-magnetic dimers even for very dilute concentrations (<0.1%) deposited at low temperatures (140K). Our data shows that this scenario holds from mono to multilayers graphene on SiC(000-1), SiC(0001) and graphite.

Hydrogen adsorption and interaction on graphitic surfaces has been extensively studied both from theoretical and experimental points of view in the last 35-40 years in different areas [1-7]. The field has gained new interest in recent years due to the appearance of graphene [8]. As widely predicted [9-11], and recently demonstrated [12], the adsorption of a single hydrogen atom on graphene leads to the emergence of an extended graphene magnetic moment of 1 Bohr magneton. Thus, a natural question that arises is whether it is possible to induce a large magnetic moment in graphene by the simple adsorption of a large number of H atoms. Previous scanning tunnelling microscopy (STM) studies have shown, the formation of different dimers and clusters on the surface of graphite and graphene when adsorbed at room temperature [13-15]. This is crucial since the magnetic moments generated by neighbouring H atoms follows very particular coupling rules: two H atoms chemisorbed on the same sublattice exhibit a ferromagnetic coupling while two H atoms on opposite sublattices are non-magnetic when in proximity [12]. Moreover, only isolated H atoms and magnetic dimers present localized states close to the Fermi energy, which is critical for transport properties [16, 17].

Despite the intensive research carried out in this field, our STM experiments reveal that it is necessary to reconsider the present understanding for atomic H adsorption on graphene surfaces. Our results show that, contrary to expectations, most of chemisorbed H atoms form non magnetic dimers even for very dilute concentrations deposited at low temperatures. Since we employed very low H doses, the probability that two H atoms are directly adsorbed on the close vicinity is negligible, This implies that H atoms must diffuse long distances on graphene even at low temperatures, where the low thermal energy prevents H diffusion between different chemisorbed positions, until they find a previously chemisorbed H atom with whom they react to form a dimer. This calls for some additional ingredient to complete the H adsorption picture, in particular for the existence of a rapid H diffusion channel on graphene. With the support of density functional theory (DFT) calculations including van der Waals forces, we point to a physisorption channel where the H is free to move, located ~3.0 Å above the graphene layer, as key to understand the final configuration of H atoms chemisorbed on graphene. To check how general this scenario is, we also carry out the experiments for graphene layers grown on different surfaces. Our data show that the physisorption channel seems to dominate the adsorption of H atoms for every system consisting of stacks of graphene layers. This holds irrespectively of the number of graphene layers, the angle of rotation between them or the doping level.

All the experimental data reported here are acquired at 5K by using a home-made low temperature scanning tunneling microscope (LT-STM) in ultra-high vacuum (UHV) conditions [18]. The data are acquired and processed using the WSxM software [19]. We carry out extensive STM experiments where atomic hydrogen is deposited at RT and 140K on graphene grown on SiC(000-1). Pristine graphene samples are prepared under UHV by graphitization of a 6H-SiC(000-1) surface [20]. We have also investigated H adsorption in HOPG surfaces, mono and bilayers of graphene on SiC(0001), graphene/Cu(111) and graphene/Ir(111) [21]. In all cases, we deposit atomic hydrogen following the procedure of refs *[12, 22]* i.e. by the thermal dissociation of H_2. The pristine graphene substrate is held at a fixed temperature during atomic H deposition and subsequently cooled down to 5K [21].

A first and quite challenging step stems in the acquisition of high enough resolution STM images to analyse the final configuration of hydrogen atoms on graphene. Following section 1b of the SOM of [12] and by comparison with DFT calculations, we are able to identify up to 10 different dimer configurations, 5 of them reported here for the first time. Figure 1 shows a representative STM image of a graphene region after room temperature atomic hydrogen deposition (see [21] for a larger region). In the image, we have highlighted some of the identified dimers. We follow ref [15] and label the dimers by a combination of the ortho (O), para (P) and meta (M) vectors (see inset in Figure 1a.). Image 1a illustrates what it is found on graphene layers after the deposition of dilute concentrations of H atoms at RT. There are 45 H atoms in this $500nm^2$ region (0.2% H coverage) 42 of them are forming non-magnetic dimers and only 3 contribute to graphene magnetism; 2 forming a magnetic dimer (outlined by a cyan circle) and 1 in a single configuration (outlined by a yellow circle). To quantitatively investigate the statistical distribution for the different H configurations observed, we perform extensive STM experiments in samples with H coverages between 0.15% and 0.3% obtained in different RT atomic H deposition experiments, see figure 1b [21]. As indicated in previous studies [13, 15], we quantitatively show here that the most common dimers on the surface are the O (13%) and P (73%) configurations. An important outcome from our study is that only a minimal amount (~5%) of the hydrogen atoms found on the sample ended up in magnetic configurations (shown in cyan), 2% as monomers and the rest forming magnetic dimers. In our STM data, there is only a 5% of H features, labelled as "unidentified", that are not able to safely assign to a defined H configuration.

To comprehend the H distribution found, we analyse the current understanding of hydrogen adsorption on graphene. When a first H atom reaches a pristine graphene layer it has to overcome a small energy barrier of 0.1-0.2 eV in order to reach the chemisorbed state. The π graphene bonds need to be broken to form a new σ bond and the physical mechanism which allows such a transition is the local deformation of the crystallographic structure by a carbon atom moving out of the graphene plane, thus transforming the sp2 hybridization to a local sp3 hybridization [23, 24]. Once the atom overcomes the barrier it gets chemisorbed with a binding energy ~0.7-1.0 eV [9, 15, 22, 25-29], a value which slightly decreases when considering the zero point energy of the C-H bond [30]. The binding energy, together with the adsorption barrier, leads to a desorption energy for a single H atom ~1-1.2 eV [27, 29, 31] which is similar but slightly lower than the migration one [29, 31-33]. Therefore, given the energy values involved for H migration, between chemisorbed sites, a hydrogen atom is not expected to travel very far on graphene when deposited at RT. Just to illustrate, following the Arrhenius expression, $\nu = \nu_{0m} e^{-E_m/k_B T}$, with E_m the migration energy and ν_{0m} the pre-exponential factor, for a low migration value E_m = 0.94 eV, [29] and a typical pre-exponential value ν_{0m} = 3·1013 Hz, [33] one expects ν~$5 \cdot 10^{-3}$ jumps/second. In our sample preparation, it takes 360 seconds from H deposition till the sample is attached to the cold finger (where it reaches 30K in only 300 seconds more) to perform STM experiments. Therefore, even in a favourable scenario for H migration -low energy barrier for migration and neglecting the possibility of desorption- the H atom would only be able to perform few jumps before its thermalization at LT. Moreover, the lower desorption energy would imply that, at room temperature, chemisorbed single hydrogen atoms will desorb more often than diffuse. Dimers exhibit a higher thermal stability [15, 22, 34-36], but the predominance of the desorption process prevents its formation via diffusion. Clustering was explained as a consequence of preferential hydrogen sticking caused by reduced or even vanishing adsorption barriers in the vicinity of previously chemisorbed hydrogen atoms [15, 22].

According to the just described scenario, one approach to maximize the number of single hydrogen atoms would be the hydrogenation of graphene at lower sample temperatures. Following the Arrhenius expression, $\nu = \nu_0 e^{-Ed/k_BT}$, with E_d the desorption or migration energy and ν_0 the pre-exponential factor, at low enough sample temperatures the desorption or migration probability of single hydrogen atoms will be negligible and graphene should present a much larger number of hydrogen monomers. In [21] we show a STM image of a graphene sample hydrogenated at 140K presenting a low H coverage of 0.15%. Contrary to our expectations, the number of single hydrogen atoms does not increase significantly, and we mostly observe dimers. This can be observed in greater detail in the statistic study shown in figure 1c. The analysis was done following the same method as for the RT experiments. We basically observe O and P dimers and the ratio P/O has increased. These results, showing that most of H atoms form dimers even when deposited at low concentrations and low temperatures, can not be understood within the present framework for hydrogen adsorption on graphene.

In order to shed light to the dynamical processes leading to the adsorption of hydrogen on graphene, we perform DFT calculations including van der Waals functionals. All the calculations that we present here are performed in a 7x7 graphene cell, with periodic boundary conditions, using a double-zeta polarized basis set and a lattice constant of 1.428 Å. We use the DRSLL functional, proposed by Dion et al. to include van der Waals interactions [37, 38]. Following ref [39], we have corrected our calculations for the basis-set superposition error (BSSE) using a posteriori counterpoise (CP) correction, to avoid unphysical overbinding due to the use of atomic orbital sets. We applied a mesh cut off of 400 Ryd and residual forces lower than 0.02 Ryd/Bohr. We use a polynomial smearing method [40] due to the rapid variation of the density of states at the Fermi level. During the calculations, the only carbon atoms not allowed to relax are the ones located at the edge of the cell. The results slightly depend on the van der Waals implementation, but they are qualitatively very similar.

We calculate the potential energy curves for the adsorption of a single hydrogen atom in three different high symmetry positions of the graphene lattice: on-top, saddle and hollow. As shown in Figure 2, the most relevant feature is the existence of a physisorption well for all the three positions. A closer look to the shape of the physisorption well, see inset of Figure 2, shows that it is almost identical for the three positions, see [21] for a closer zoom in. It presents a minimum at ~60 meV below the energy required to reach the chemisorbed state. This means that once a hydrogen atom enters the physisorption well, it will be able to freely move laterally along the sample without feeling the presence of the carbon lattice underneath. The physic governing the physisorption well is dominated by van der Waals forces. Therefore, the weak corrugation of the potential well is in inherent to the nature of the van der Waals forces, which are rather long ranged. At those distances, the Hydrogen atom is essentially insensitive to the details of the underlying carbon lattice. This can be appreciated in [21], where it can be seen that the graphene lattice does not feel the presence of the H atom while the H atom stays in the physisorption region (C atoms do not modify their positions until the Hydrogen atom approach at a distance ~2.1Å). The existence of this physisorption channel has already been considered in the formation of molecular hydrogen in the interstellar medium, where the low temperatures would deactivate the chemisorption process. Moreover, it was measured by means of H and D scattering experiments in 1980, obtaining a value around 40 meV [41], and different types of calculations also resulted in a physisorption well with similar values [23, 39, 42]. However, the presence of a physisorption channel is routinely neglected when addressing the hydrogenation of graphene at higher temperatures.

If we now take into account the existence of an active physisorption channel as our DFT calculations point out, the adsorption process leading to the final configuration of hydrogen atoms on graphene samples differs from the one previously described. First, a hydrogen atom approaches the graphene surface until it enters the physisorption channel at a distance of ~3.0 Å. As illustrated in fig 2, once it is physisorbed, it moves laterally over the surface without encountering any barrier hindering its displacement parallel to the surface. While the hydrogen atom is moving, it can either overcome the adsorption barrier after some attempts or end up desorbing or attaching to a reactive surface defect. Once a hydrogen atom is chemisorbed, the adsorption energy barriers around it are affected, reducing their value and even disappearing for some specific lattice positions [15, 22]. Then, as illustrated in Fig 3c, when a second hydrogen atom enters the physisorption channel, it feels a modified energy landscape, where the height and even the existence of the adsorption barriers depend on the specific site of the graphene lattice with respect to the already chemisorbed hydrogen atom.

These position dependent changes in the adsorption barrier can be seen as an increment of the reactivity of the graphene region surrounding the chemisorbed hydrogen atom. In order to check whether these changes would explain the H distribution found on our samples, we calculate the adsorption energy curves of a second hydrogen atom on different atomic sites and along several high symmetry directions close to the already chemisorbed one. In Figure 3a we show three representative positions: O, P and POP. In the case of the POP dimer, due to the large distance to the chemisorbed hydrogen atom, its adsorption barrier is basically the same as in the case of a single hydrogen atom. For the case of the P dimer and its surroundings (blue shadowed regions in Fig. 3c) the adsorption barrier disappears meaning that when a hydrogen atom gets close enough to the P position, it will be chemisorbed with essentially a 100% probability. This absence of adsorption barrier would be in good agreement with the P dimer being the most observed in our samples despite having a similar adsorption energy of ~2 eV as the O dimer, see Figures 3a and [15, 21, 22, 34-36]. Such a large energy gain can be understood in simple terms by noticing that the H adsorption creates a localized state at the Fermi energy occupied by a single electron and mainly localized on the opposite sublattice with respect to H adsorption. When two H adsorb on different sublattices, as for the O and P dimers, two states are created on different sublattices, these hybridize creating a bonding state that is now occupied by the two electrons forming a singlet state. The O dimer is a peculiar case, there is still an adsorption barrier but its value has strongly decreased. This facilitates the chemisorption and formation of the O dimer but leaves open the possibility for the hydrogen atom to continue moving along the physisorption channel. In Figure 3b we show both possibilities for a hydrogen atom moving along the physisorption channel from a hollow position towards a chemisorbed hydrogen atom through the O site. In red, the hydrogen atom overcomes the adsorption barrier and gets chemisorbed forming an O dimer. In green, the hydrogen atom continues along the physisorption channel without overcoming the barrier, until it reaches the O site. At this point, the hydrogen atom reacts with the chemisorbed one forming a hydrogen molecule and thus desorbing. Both possibilities are illustrated by the two O and O(H_2) trajectories shechted in Fig 3c. This is also consistent with our data showing the increase of the P/O dimers ratio that we find at 140K, see Figs 1b,c. While the lower thermal energy decreases the probability of a second hydrogen atom to overcome the adsorption barrier to form the O dimer, the absence of adsorption barrier leaves the probability to form the P dimer essentially unaltered. Finally, our calculations show that when a physisorbed hydrogen atom gets close enough to the chemisorbed one (green shadowed region in Fig. 3c), both hydrogen atoms react forming a H_2 molecule which desorbs from the graphene surface. H_2 formation and desorption also happens when two H atoms travelling along the physisportion channel meet each other.

Additional experimental evidence about the existence of a rapid diffusion channel for hydrogen atoms on graphene can be found on grain boundaries. Grain boundaries are line defects formed at the frontier between graphene regions with different lattice orientations [21]. They consist of a series of non-hexagonal carbon rings which are known to be more chemically reactive than pristine graphene [43-45]. Therefore, physisorbed hydrogen atoms fastly diffusing over the clean graphene surface are expected to get trapped while crossing those line defects. Our STM data show that this is the case, with hydrogen atoms decorating grain boundaries, even when very low concentrations are deposited at low temperatures (see Figure 4a and [21]).

Finally, to check the universality of the scenario here proposed, we investigate the adsorption of low concentrations of atomic hydrogen on graphene layers on top of different substrates. Our STM data show that the physisorption channel seems to be active for well enough decoupled graphene layers and for graphene layers on top of other graphene layers, independently of the number of layers, the angle of rotation between them or the doping level (at least for moderate values). We have measured HOPG surfaces, 1 to 6 layers of graphene on SiC(000-1) and mono and bilayers of graphene on SiC(0001) [21]. On all these systems, following an identical experimental procedure as previously described, our STM images show essentially the same final configuration of hydrogen atoms, with the majority of them forming P and O non-magnetic dimers, see figures 4b-d and [21]. Interestingly, the situation is completely different for graphene on metallic substrates. There, even for relatively well decoupled graphene layers, the final configuration of hydrogen atoms strongly depends on the specific metal: while periodic arrays of hydrogen clusters form on the bright regions of the graphene/Ir(111) moiré [21], [46] opening a gap in its electronic band structure, isolated hydrogen atoms are mostly found for graphene/Cu(111) [21], [47]. Alternatively, changing the adsorbate nature could also give rise to isolated sp^3 defects on graphene [48, 49]. Our DFT calculations show that this seems to be the case for the adsorption of F atoms. The potential energy curve for the adsorption of a single F atom on graphene shows that F reaches a stable chemisorption state (~1.2 eV) without the need to overcome any energy barrier [21]. Thus, one could expect that mostly isolated F atoms would be found on graphene samples after fluorination.

To summarize, our results show the existence of a physisorption channel dominating the adsorption of H atoms on many graphene systems. The physisorption well is governed by van der Waals forces, presenting a very weak potential corrugation over the whole graphene lattice. This is particularly relevant for experiments aiming to tune graphene properties by its macroscopic hydrogenation. Our results demonstrates that on those systems only a very minor amount of the H atoms adsorbed on graphene will be unpaired, which has strong implications both for transport and magnetic properties. Moreover, we show the persistence of an active physisorption channel at relative high temperatures, when H atoms would have enough thermal energy as to eventually reach the chemisorption state. This keeps active the catalytic role of those graphene surfaces, with the formation of molecular hydrogen when two H atoms travelling along the physisorption channel meet each other.

Figures

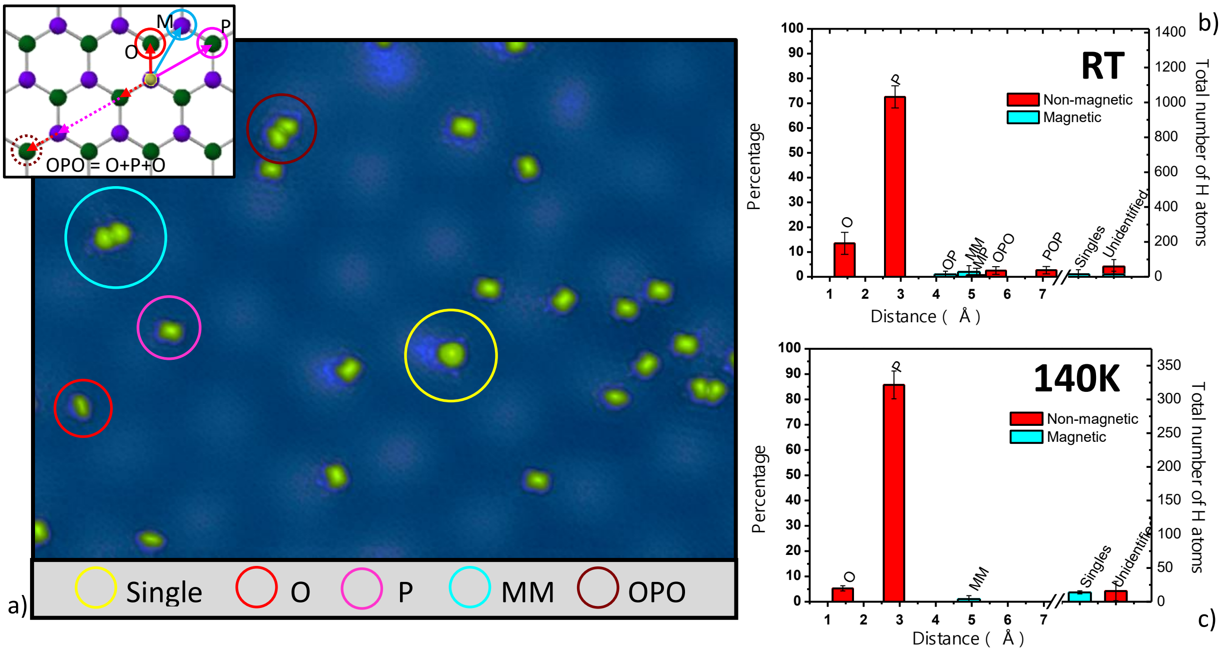

Figure 1. a) STM image of the graphene/SiC(0001) sample after RT hydrogenation. Some hydrogen configurations have been highlighted. Dimers are labelled by a combination of the ortho (O), para (P) and meta (M) vectors, see upper-left inset. Image measured at 5K, size 25x20 nm², Vbias=-0,4eV, It=50 pA. b) Upper/bottom histogram: statistical distribution of hydrogen atoms in each dimer configuration after RT/140K hydrogenation. “Unidentified” refers to clusters of H atoms or some pairs which were not recognisable.

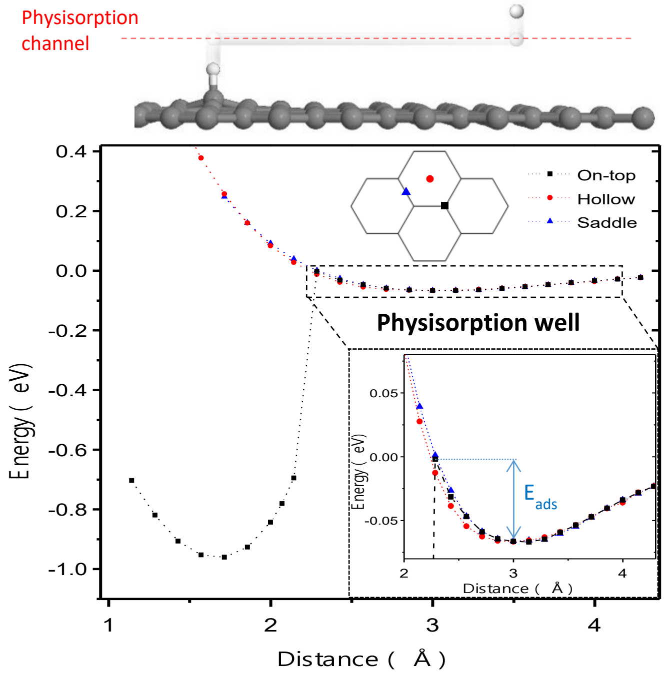

Figure 2. Energy-distance curves of the adsorption of a single hydrogen atom on 3 different positions of the graphene lattice: on-top, hollow and saddle. The energy is referred to the case of hydrogen and graphene being far apart. Inset: zoom in of the physisorption well. Upper drawing illustrates the adsorption path followed by a hydrogen atom towards the chemisorption state.

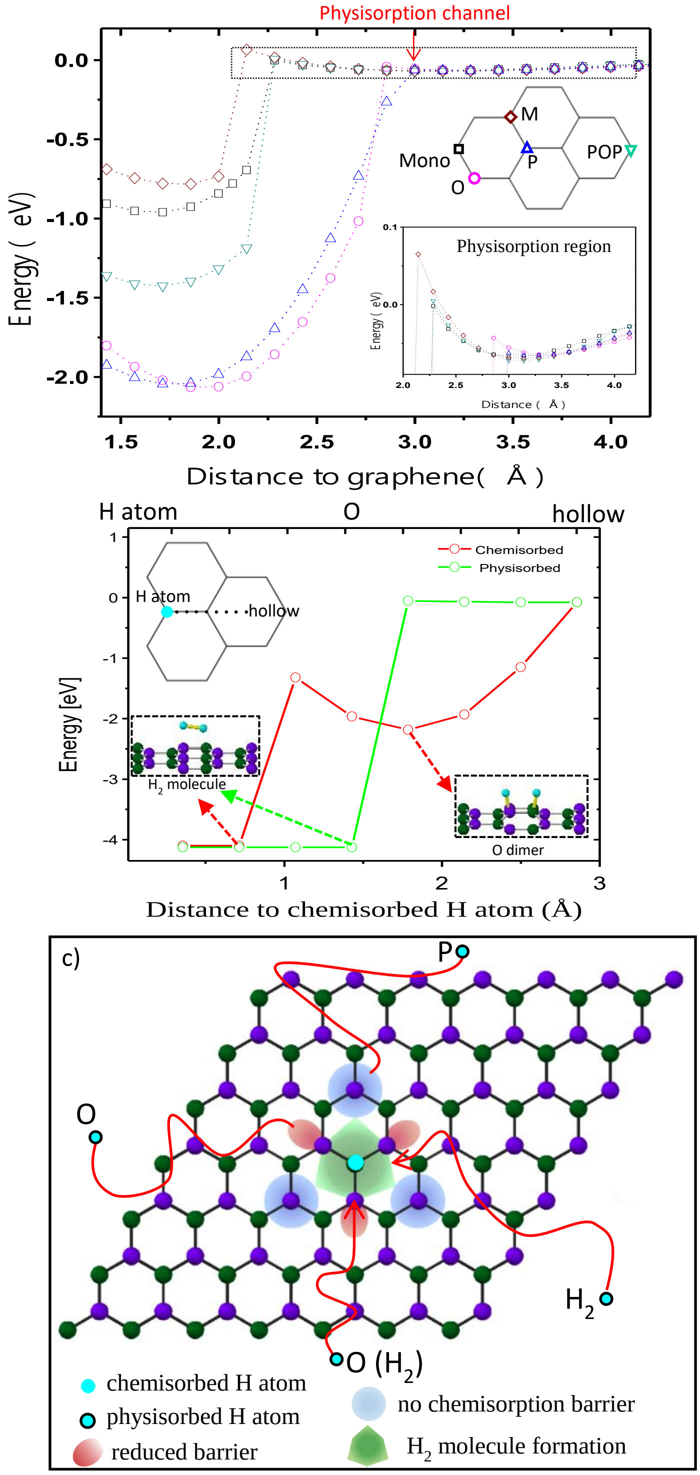

Figure 3: a) Energy-distance curves for the adsorption of a second hydrogen atom diffusing along the physisorption channel in the vicinity of a previously chemisorbed one. 4 different neighboring carbon lattice sites are considered. Inset: zoom in around the physisorption region to show the different adsorption barriers. b) Energy of a second hydrogen atom as it approaches from a hollow to the nominal O position via the physisorption (green curve) or the chemisorption channel (red curve). c) Scheme illustrating the adsorption of a second hydrogen atom in the vicinity of a chemisorbed atom. Red lines represent four different physisorption paths for the hydrogen atom to

get close to the chemisorbed one. Depending on the trajectory, O dimer, P dimer or a H_2 can result.

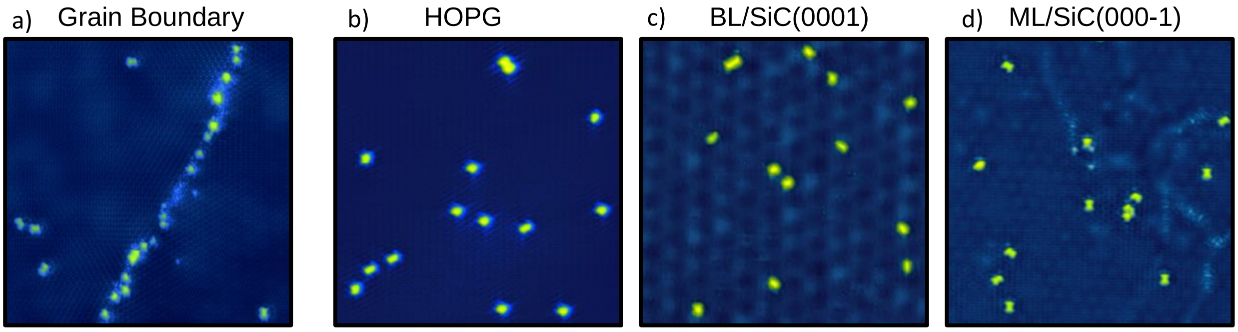

Figure 4. a) STM image of a graphene grain boundary heavily populated by hydrogen atoms. (b-d) STM images after the atomic hydrogenation of graphene layers on different substrates. All (b-d) images, with sizes of 20x20 nm^2 and hydrogen concentrations of ~0.17%, show most H atoms forming O and P dimers. Hydrogenation was performed at 140K in all cases.

Acknowledgments:

This work was supported by Spain's Ministerio de Economía y Competitividad under grants; PCIN-2015-030; FIS2015-64886-C5-5-P, MDM-2014-0377 and FIS2016-80434-P, by AEI and FEDER under projects MAT2016-80907-P and MAT2016-77852-C2-2-R (AEI/FEDER, UE), by the Fundación Ramón Areces, by the European Union through the FLAG ERA program and structural funds and by the Comunidad de Madrid MAD2D-CM program under grant S2013/MIT-3007.

References

[1] R. Dovesi *et al.*, Journal of Chemical Physics **65**, 3075 (1976).
[2] V. Pirronello *et al.*, Astrophysical Journal **475**, L69 (1997).
[3] L. Hornekær *et al.*, Science **302**, 1943 (2003).
[4] V. Pirronello *et al.*, Astronomy & Astrophysics **344**, 681 (1999).
[5] L. Schlapbach, and A. Zuttel, Nature **414**, 353 (2001).
[6] V. Meregalli, and M. Parrinello, Applied Physics a-Materials Science & Processing **72**, 143 (2001).
[7] M. Mayer *et al.*, Journal of Nuclear Materials **290**, 381 (2001).
[8] K. S. Novoselov *et al.*, Science **306**, 666 (2004).
[9] P. O. Lehtinen *et al.*, Physical Review Letters **93**, 187202 (2004).
[10] V. M. Pereira *et al.*, Physical Review Letters **96**, 036801 (2006).

[11] O. V. Yazyev, and L. Helm, Physical Review B **75**, 125408 (2007).
[12] H. González-Herrero *et al.*, Science **352**, 437 (2016).
[13] L. Hornekaer *et al.*, Physical Review Letters **96**, 156104 (2006).
[14] P. Merino *et al.*, Langmuir **31**, 233 (2015).
[15] Z. Sljivancanin *et al.*, Journal of Chemical Physics **131**, 084706 (2009).
[16] N. Leconte *et al.*, Acs Nano **5**, 3987 (2011).
[17] F. Gargiulo *et al.*, Physical Review Letters **113**, 246601 (2014).
[18] M. M. Ugeda *et al.*, Physical Review Letters **104**, 096804 (2010).
[19] I. Horcas *et al.*, Review of Scientific Instruments **78**, 013705 (2007).
[20] F. Varchon *et al.*, Physical Review B **77**, 165415 (2008).
[21] *see Supplementary Material*.
[22] L. Hornekaer *et al.*, Physical Review Letters **97**, 186102 (2006).
[23] L. Jeloaica, and V. Sidis, Chemical Physics Letters **300**, 157 (1999).
[24] X. W. Sha, and B. Jackson, Surface Science **496**, 318 (2002).
[25] M. Moaied, J. V. Alvarez, and J. J. Palacios, Physical Review B **90**, 12 (2014).
[26] X. Sha, and B. Jackson, Surface Science **496**, 318 (2002).
[27] V. V. Ivanovskaya *et al.*, The European Physical Journal B **76**, 481 (2010).
[28] V. A. Borodin *et al.*, Physical Review B **84**, 075486 (2011).
[29] Y. Ferro *et al.*, The Journal of Chemical Physics **120**, 11882 (2004).
[30] I. Brihuega, and F. Yndurain, Journal of Physical Chemistry B **122**, 595 (2018).
[31] H. McKay *et al.*, Physical Review B **81**, 075425 (2010).
[32] T. O. Wehling, M. I. Katsnelson, and A. I. Lichtenstein, Physical Review B **80** (2009).
[33] M. Moaied *et al.*, Physical Review B **91**, 155419 (2015).
[34] N. Rougeau, D. Teillet-Billy, and V. Sidis, Chemical Physics Letters **431**, 135 (2006).
[35] Y. Ferro *et al.*, Physical Review B **78**, 085417 (2008).
[36] S. Casolo *et al.*, Journal of Chemical Physics **130**, 054704 (2009).
[37] M. Dion *et al.*, Physical Review Letters **92**, 246401 (2004).
[38] G. Román-Pérez, and J. M. Soler, Physical Review Letters **103**, 096102 (2009).
[39] M. Bonfanti *et al.*, The Journal of Physical Chemistry C **111**, 5825 (2007).
[40] M. Methfessel, and A. T. Paxton, Physical Review B **40**, 3616 (1989).
[41] E. Ghio *et al.*, The Journal of Chemical Physics **73**, 556 (1980).
[42] H. M. Cuppen, and L. Hornekaer, The Journal of Chemical Physics **128**, 174707 (2008).
[43] O. V. Yazyev, and S. G. Louie, Nature Materials **9**, 806 (2010).
[44] A. Salehi-Khojin *et al.*, Advanced Materials **24**, 53 (2012).
[45] P. Yasaei *et al.*, Nature Communications **5** (2014).
[46] R. Balog *et al.*, Nature Materials **9**, 315 (2010).
[47] H. Gonzalez-Herrero *et al.*, Acs Nano **10**, 5131 (2016).
[48] J. O. Sofo *et al.*, Physical Review B **83**, 081411(R) (2011).
[49] F. Yndurain, Physical Review B **90**, 245420 (2014).